X-620-68-200
PREPRINT

NASA TM X-63217

PRELIMINARY RESULTS OF VENUS OBSERVATIONS BETWEEN 8 AND 13μ

R. HANEL
M. FORMAN
T. MEILLEUR
G. STAMBACH

GPO PRICE $ _____
CFSTI PRICE(S) $ 3.00
Hard copy (HC) _____
Microfiche (MF) 1.65
ff 653 July 65

MAY 1968

GSFC
GODDARD SPACE FLIGHT CENTER
GREENBELT, MARYLAND

X-620-68-200

PRELIMINARY RESULTS OF VENUS OBSERVATIONS BETWEEN 8 AND 13 μ

R. Hanel, M. Forman,
T. Meilleur*, and G. Stambach

May 1968

Goddard Space Flight Center
and
*Consultants and Designers, Inc.

PRELIMINARY RESULTS OF VENUS OBSERVATIONS BETWEEN 8 AND 13 μ

R. Hanel, M. Forman,
T. Meilleur, and G. Stambach

ABSTRACT

The emission spectrum of Venus has been observed between 750 cm^{-1} and 1250 cm^{-1} from the 61 inch Harvard Observatory telescope using a Michelson interferometer capable of resolving one wavenumber. A preliminary analysis confirms a broad absorption-like feature near 890 cm^{-1} but evidence of the 960 and 1060 cm^{-1} CO_2 bands is weak if observable at all. The 791 cm^{-1} CO_2 Q branch seems to be stronger in the Venus spectra than in the lunar comparison spectrum. The measured brightness temperature of about 250°K is slightly higher than most previous estimates.

CONTENTS

TABLE OF SYMBOLS

$B_\nu(T)$	Planck function at wavenumber ν and temperature T (Watt cm^{-2} $ster^{-1}$ cm)
I_ν	specific intensity (Watt cm^{-1} $ster^{-1}$)
k_ν	absorption coefficient per gram of H_2O (g^{-1} cm^2)
m	air mass
p/p_0	normalized atmospheric pressure
S_ν	specific intensity at the coude focus (Watt cm^{-1} $ster^{-1}$)
T	temperature (degrees Kelvin)
z	vertical coordinate (km)
ΔV	difference spectrum between planet and adjacent sky (Watt cm^{-1} $ster^{-1}$)
ϵ	emissivity of telescope
ν	wave number (cm^{-1})
ρ	water vapor density (g cm^{-3})
τ_{atm}	atmospheric transmittance
τ_{tele}	transmittance of telescope
Ω_v	solid angle of planet (ster)
Ω_i	solid angle of instrument (ster)

PRELIMINARY RESULTS OF VENUS OBSERVATIONS BETWEEN 8 AND 13μ

INTRODUCTION

This paper reports preliminary results obtained from observations of Venus in the 750 - 1250 cm^{-1} region by Fourier spectroscopy techniques. The thermal emission spectrum of Venus has been observed in this spectral region previously. Early radiometric work by Coblentz, Lampland, Pettit, and Nicholson has been summarized for example by Pettit (1961). More recently Sinton and Strong (1960) obtained spectra of Venus at a resolving power of 30 and 150 using a prism and a grating spectrometer on the 200" telescope at Mt. Palomar. Sinton (1962), Murray et. al. (1963), and Westphal et. al. (1965) report on observations of the brightness temperature in this spectral range. Low (1968) has obtained spectra at a resolving power of 50 with the aid of a filter radiometer. Estimates on the brightness temperature of Venus vary considerably from as low as 210°K by Westphal et. al. to values as high as 257°K observed on one day by Sinton.

OBJECTIVES

The emission spectrum of Venus contains information on the thermal structure of the atmosphere near and above the upper limit of the clouds. It would be desirable to observe the total infrared emission spectrum from the near infrared to the microwave region; however, only a small range from 750 to 1250 cm^{-1} (8 - 13μ) is accessible to an observer at sea level. It would also be desirable to observe the illuminated and dark side of Venus separately; however, energy and seeing considerations permitted observations of the whole planetary disk only.

In combination with theoretical models, see for example Bartko and Hanel (1968), the emission spectrum permits an insight into the physical conditions of the atmosphere. Besides these more general goals, three rather specific objectives may be pursued.

The first objective concerns the structure of the CO_2 bands at 1060, 960, and 791 cm^{-1}. With a resolving power of 1000, individual lines may just be observable. Information on the atmospheric lapse rate may be obtained from the appearance of these bands.

The second objective was to reexamine the broad absorption like feature near 890 cm^{-1} which appears in the low resolution but not in the high resolution spectra of Sinton and Strong. If the phenomenon is a reality, it may yield information on the clouds since at this spectral range, carbon dioxide is relatively transparent, and the cloud particles are probably the emitting matter.

The third objective was to infer the brightness temperature of Venus from an absolute measurement of the spectral flux. Previous estimates of the brightness temperature show a considerable spread.

INSTRUMENTATION

To this end, a Michelson type interferometer was constructed which can resolve about one wave number in the 750 - 1250 cm^{-1} region; however, in most instances a slightly lower resolution was used. The instrument is operated in a dual input, differential mode and uses two mercury doped germanium detectors at liquid helium temperatures to record radiation transmitted as well as reflected by the beam splitter. In contrast to instruments of similar nature (Felgett 1958, Connes 1966) the same area of the beamsplitter is used for separation and recombination of all interacting beams, but the beams occupy different parts of the permissible solid angle. The sampling command is derived from a fringe control interferometer which operates in the same space as the prime interferometer but uses a different coating applied only to the center of the potassium bromide substrate of the beamsplitter. Neither internal nor external modulation is employed. A commercially available,* servo controlled unit provided a reliable means of displacement for the Michelson mirror. The signals from both detectors were amplified, electrically filtered, digitized to 12 bits, and recorded in computer compatible format on magnetic tape. The apodisation, Fourier transformation, calibration, and finally the combining of both channels was done in a digital computer. The spectra shown have been generated by an automatic plotter from the computer output. The design and performance of this instrument will be discussed elsewhere.

The interferometer was adapted to the coudé focus of the 61" telescope at the Harvard Observatory in Massachusetts. Figure 1 shows a simplified diagram of the optical path for one detector. The planetary image at the coudé focus is formed again at two prismatically shaped mirrors at the entrance and exit of the interferometer, and finally appears at an aperture in front of a field lens. This aperture defines the field of view. It was chosen about twice the diameter of the planetary image. The ratio of the aperture area to the image size enters the estimate of the planetary brightness temperatures.

The image of the primary telescope mirror appears at the first F34/F4 conversion mirror (f = 17.5 cm), then at the flat interferometer mirrors, again at the second conversion mirror (f = 13.6 cm), and finally at the detector. This

*Idealab Inc., Franklin, Mass.

design principle assures a uniform sensitivity across a well defined field of view. Another advantage is the lack of obscuration due to the fringe control interferometer which occupies the central area of the beam cross section in the interferometer. The fringe control elements become hidden behind the obscuration caused by the secondary telescope mirror.

OBSERVATIONS

During two periods of time, from September 23 to October 5 and from October 22 to October 31, 1967, the emission from Venus and the moon was observed whenever conditions permitted. During these observations, the sky emission with and without the telescope, and radiation from blackbodies were also recorded for the purpose of establishing a basis for an absolute calibration. This report shows data from October 30 only. On that date, a complete set of data was obtained within a short time period under good seeing conditions. In most cases, each source was observed 16 times in succession for 21 seconds per observation. Each interferogram, the output of the detectors, was transformed into a raw spectrum, and the average spectrum and sample standard deviation was computed for each group. This procedure provides a means of assessing the magnitude of random errors in the results. A typical uncalibrated average spectrum representing an observation time of 5.6 minutes and the associated sample standard deviation is shown in Figure 2. The other detector generated a similar set simultaneously.

For certain periods of time, the instrument was exposed to two blackbodies, one at room temperature and the other one at a warmer temperature (45°C). Planetary, lunar, and atmospheric spectra were then normalized to the blackbody spectra. Hence, the spectra, s_ν, could be calibrated in radiometric units at a point just behind the field mirror located at the coudé focus. While observing the planet through the telescope, this signal may be represented at each resolved wavenumber interval by:

$$s_\nu = \left(I_v \frac{\Omega_v}{\Omega_i} \tau_{atm} + \int_1^{\tau_{atm}} B_\nu (T)\, d\tau \right) \tau_{tele} + \epsilon B\left(T_{tele}\right) \qquad (1)$$

The Flux from Venus $I_v \Omega_v$ divided by the solid angle of the instrument Ω_i, is attenuated by the earth's atmosphere, and augmented by the thermal emission from the atmosphere. This quantity is incident at the primary mirror of the telescope. The telescopic transmission is represented by τ_{tele}, and the last term accounts for the emission from the telescope. After each planetary and

lunar observation the sky emission next to the object was recorded. The difference of the spectra removes telescopic and atmospheric emission, at least in first order, but not the effect of the transmission factors. The difference spectrum for Venus may be written

$$\Delta V = I_v \frac{\Omega_v}{\Omega_i} \tau_{atm} \tau_{tele} \qquad (2)$$

Observed difference spectra of Venus and of the moon are shown in Figures 3 and 4. The Venus difference spectrum was multiplied by Ω_i/Ω_v which was equal to 3.46 in this case. Lunar observations were made when the moon was close to Venus, so that both objects could be observed through nearly the same air mass. A relatively homogeneous area in the Oceanus Procellarum near the illuminated part of the lunar equator was chosen for comparison. The ratio of the Venus difference spectrum and the lunar difference spectrum should remove the effects of the atmospheric as well as telescopic transmission. The ratio shown in Figure 5 seems to confirm this approximately; all of the strong telluric lines have been reduced between 750 and 1000 cm^{-1}, the most reliable part of the spectrum.

In addition to the measurements just discussed, an attempt was made to determine the planetary flux in radiometric units. The direct method used does not involve other objects such as the moon or the sun although the same technique was applied to the lunar data as a check. The direct method is based on an experimental determination of the telescopic as well as atmospheric transmission functions τ_{tele} and τ_{atm}. The ratio of solid angles Ω_i/Ω_v which enters the equation also has already been mentioned.

As shown in Figure 6 the telescope transmission was determined by comparing the line strength in the spectrum of the sky background while observing the sky near the planet through the telescope (1) to the same sky background observed without the telescope (4). Two additional flat mirrors (G and F) served to channel into the interferometer radiation from the same spot as observed by the telescope, but of course with a larger solid angle. The absolute calibration was performed near the meridian passage of Venus at elevation angles close to 50°. It is assumed that the sky background in this region was homogeneous and fairly constant during the 90 minute period involved.

The transmission of the two flat auxiliary mirrors F and G was determined by comparing the lines in the sky background directly overhead with (3) and without (2) the two mirrors. Their combined transmission was found to be 0.947. The telescope transmission includes the reflectivity of the primary, secondary, and tertiary as well as losses due to the first gold covered flat mirror (D) at the

end of the polar axis and the field mirror (E) at the coudé focus. Furthermore, the telescope transmission includes losses in signal caused by obscurations in excess of those already present in the interferometer, and by residual alignment errors. It is assumed that the second mirror (D) and mirror (H) have identical properties. The mirror (H) served also to reflect blackbody radiation into the interferometer during the calibration cycles.

The effective telescope transmission was found to be about 0.75 near 800 cm^{-1} and only 0.45 near 1200 cm^{-1}. This relatively strong wavenumber dependence was not expected, however, its reality was tested by determining the brightness temperature of the moon. The moon showed essentially the same values near 800 cm^{-1} as well as 1200 cm^{-1}. The wavenumber dependence of the telescope transmission may have been caused by pollen or other particles of a critical size which had accumulated in time on the primary mirror.

The atmospheric transmission was determined from sky spectra and radiosonde data. The vertical downward intensity of the sky is shown in Figure 7. The attempt to determine the atmospheric transmission was restricted to spectral regions in between the strong absorption lines. In these narrow windows, the absorption is caused by the water vapor continuum, by very weak lines, and by aerosols.

The downward intensity at the rather transparent regions may be expressed by

$$I_\nu = \int_0^\infty B_\nu \, T(z) \, e^{-\int_0^z k_\nu \frac{p}{p_0} \rho dz} \, k_\nu \, \frac{p}{p_0} \rho \, dz \, . \qquad (3)$$

The radiosonde launched nearly simultaneous with the observations of the spectra provided the atmospheric temperatures $T(z)$ up to 36 km and the relative humidity up to 8 km.

The temperatures were used to compute the value of the Planck function for different altitudes; the relative humidities were converted into mixing ratios to determine $\rho(z)$ for water vapor. The ratio p/p_0 in Equation 3 accounts for the pressure dependence of the line width of the strong lines outside the range which are partly responsible for the continuum absorption. A temperature correction was not applied. The absorption coefficient k_ν was determined for each window interval of interest by numerically integrating Equation 3 up to an altitude of 11.5 km for several values of k_ν and selecting the one which gave the intensity observed without auxiliary mirrors, case (2) in Figure 6. The values found

are given in Table 1. They are similar to those measured by Roach and Goody (1958) and somewhat higher then those of Bignell et. al. (1963). This may be expected since the coefficients of the latter group refer to water vapor only. Then the atmospheric transmission was computed from

$$\tau_{atm} = e^{-\int_0^\infty k_\nu m \frac{P}{P_0} \rho \, dz} \tag{4}$$

where m is the air mass; 1.3 for a 50° elevation angle. The effective telescopic and atmospheric transmissions are shown in Figure 8.

Finally, the Venus and lunar spectra shown in Figures 3 and 4 were divided by the telescopic and atmospheric transmission functions and the result was plotted, Figure 9.

PRELIMINARY CONCLUSIONS

By inspecting the spectra of Venus and the Moon, and their ratio, the following conclusions may be drawn:

(1) The 1060, 960, and 791 cm^{-1} bands on Venus appear to be very weak if visible at all. More spectra will have to be analyzed and a correlation analysis will have to be applied to reach a firmer conclusion. The Q branch of the 791 cm^{-1} (12.6μ) CO_2 band appears to be stronger then the adjacent telluric water lines in the Venus spectrum and weaker in the lunar spectrum indicating a positive lapse rate ($dT/dz < 0$) at the level of formation of this branch in the atmosphere of Venus.

(2) The broad absorption-like feature centered at 890 cm^{-1} (11.2μ) is apparent in the spectrum of Venus but absent in the lunar spectrum. This observation confirms the existence of this phenomenon. The feature may be caused by a residual ray effect in the material composing the clouds.

(3) The observed brightness temperatures are higher then those of Murray et. al., Westphal, et. al., Sinton and Strong, and Low, but are in agreement with some of the values reported by Sinton.

The analysis of further data and calculations of the probable error are in progress and will be reported elsewhere.

ACKNOWLEDGMENT

At the suggestion of Dr. R. Goody from Harvard University, observation time was requested at the Harvard Observatory; we are very grateful for this suggestion. We are very much indebted to the Astronomy Department of the Harvard University, especially to Dr. Liller, Dr. Danziger, and the observatory staff for making observation time and assistance available. The NASA Electronic Center in Boston provided computer time for pilot runs. We are also indebted to the Air Force, Cambridge Research Laboratory for the launching of radiosondes at specified times. Mr. Bartko participated in the early planning and Mr. Prichard from Idealab, Inc. and Mr. Gerstle from Radiation, Inc. gave us assistance at short notice. Last but not least, we are grateful to Mr. A. Simmons for his efforts in computer programming and to many individuals at GSFC.

REFERENCES

1. Bartko, F. and Hanel, R. A., 1968, Astrophys. Jour., Vol. 151, pp. 365-378.

2. Bignell, K., Saidy, F., and Sheppard, P., 1963, J.O.S.A., Vol. 53, No. 4, pp. 466-479.

3. Connes, Janine and Pierre, 1966, J.O.S.A., Vol. 56, No. 7, pp. 896-910.

4. Fellgett, P., 1958, Journal de Physique et le Radium, Vol. 19, March, p. 237.

5. Low, F., 1968, Second Arizona Conference on Planetary Atmospheres: "The Atmosphere of Venus," Tucson.

6. Murray, B. C., Wildey, R. L., and Westphal, J. A., 1963, Geophys. Res., Vol. 68, No. 16, pp. 4813-4818.

7. Pettit, E., 1961, The Solar System, Vol. III; Planets and Satellites, Kuiper, G. P., and Middlehurst, B. M., ed. Chapter 10; The University of Chicago Press.

8. Roach, W. T., and Goody, R. M., Quat. J. Roy. Met. Soc., 1958, 84 pp. 319-333.

9. Sinton, 1962, Mem. Soc. Royal des Sciences, Liege 5 ser. 7.300.

10. Sinton, W. M. and Strong, J., 1960, Astrophys. Journal, 131, pp. 470-490.

11. Westphal, J. A., Wildey, R. L., Murray, B. C., 1965, Astrophys. Journal, Vol. 142, pp. 799-802.

Table 1

Empirical atmospheric absorption coefficients derived from the sky emission spectrum. The transmission of the earth atmosphere calculated with these coefficients refers to 1 to 3 cm^{-1} wide intervals between the strong water vapor lines. It is assumed that aerosols have about the same vertical distribution as water vapor. Residual CO_2 or N_2O absorption will cause small errors in some intervals.

ν (cm^{-1})	k_ν (g^{-1} cm^2)
773	.35
781	.29
788	.27
800	.31
805	.29
812	.26
820	.26
832	.25
845	.26
860	.27
869	.27
875	.26
900	.26
912	.27
926	.27
960	.27
986	.27
1070	.34
1095	.25
1105	.23
1110	.24
1116	.25
1130	.22
1140	.27
1160	.25
1170	.29
1182	.26
1192	.27

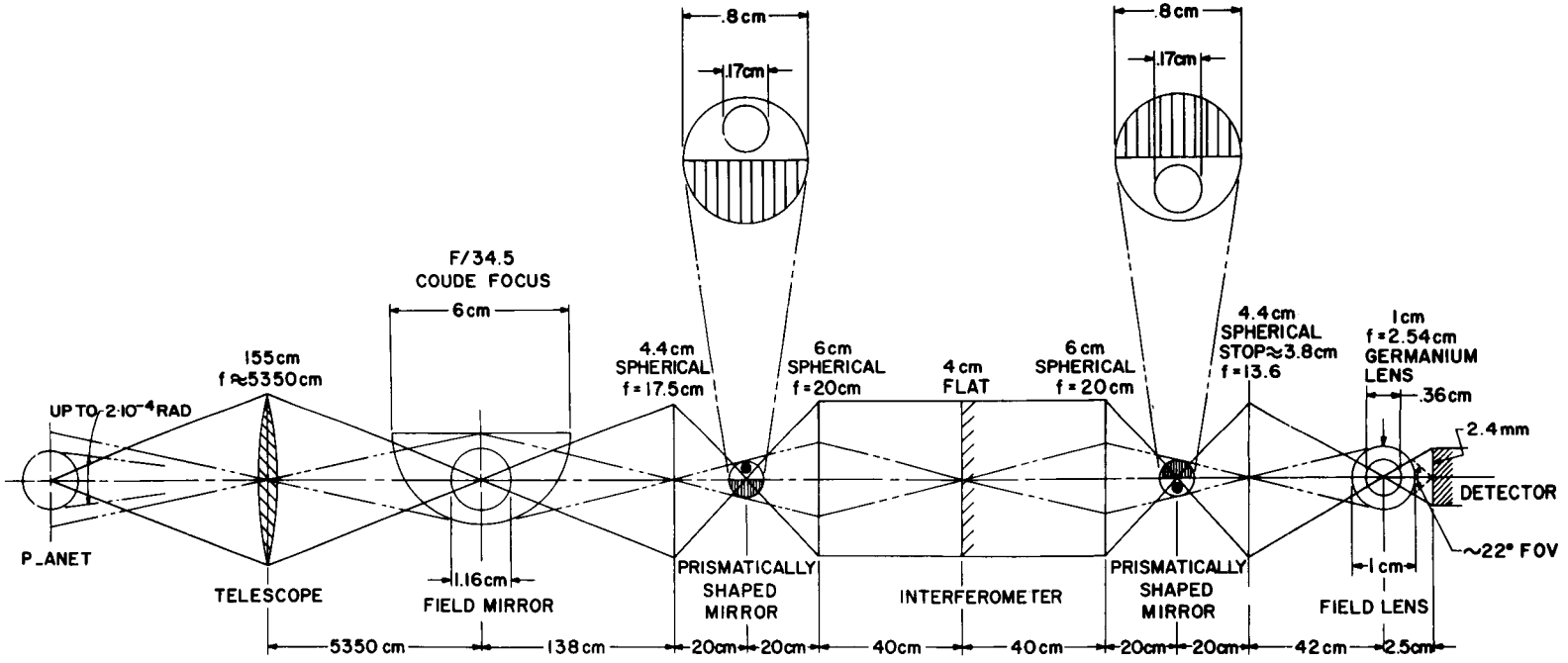

Figure 1. Schematic diagram of the optical path for one detector. The telescope is symbolized by a single element. The planetary image at the semi-circular field mirror at the coudé focus was as large as 1.16 cm for the early observation period and 0.725 cm for the second period. Diffraction causes a small increase in the image size. Although shown "on axis," the prismatically shaped mirror was positioned so that the planetary image formed on one face of the prism as indicated by the dot and the enlargement above.

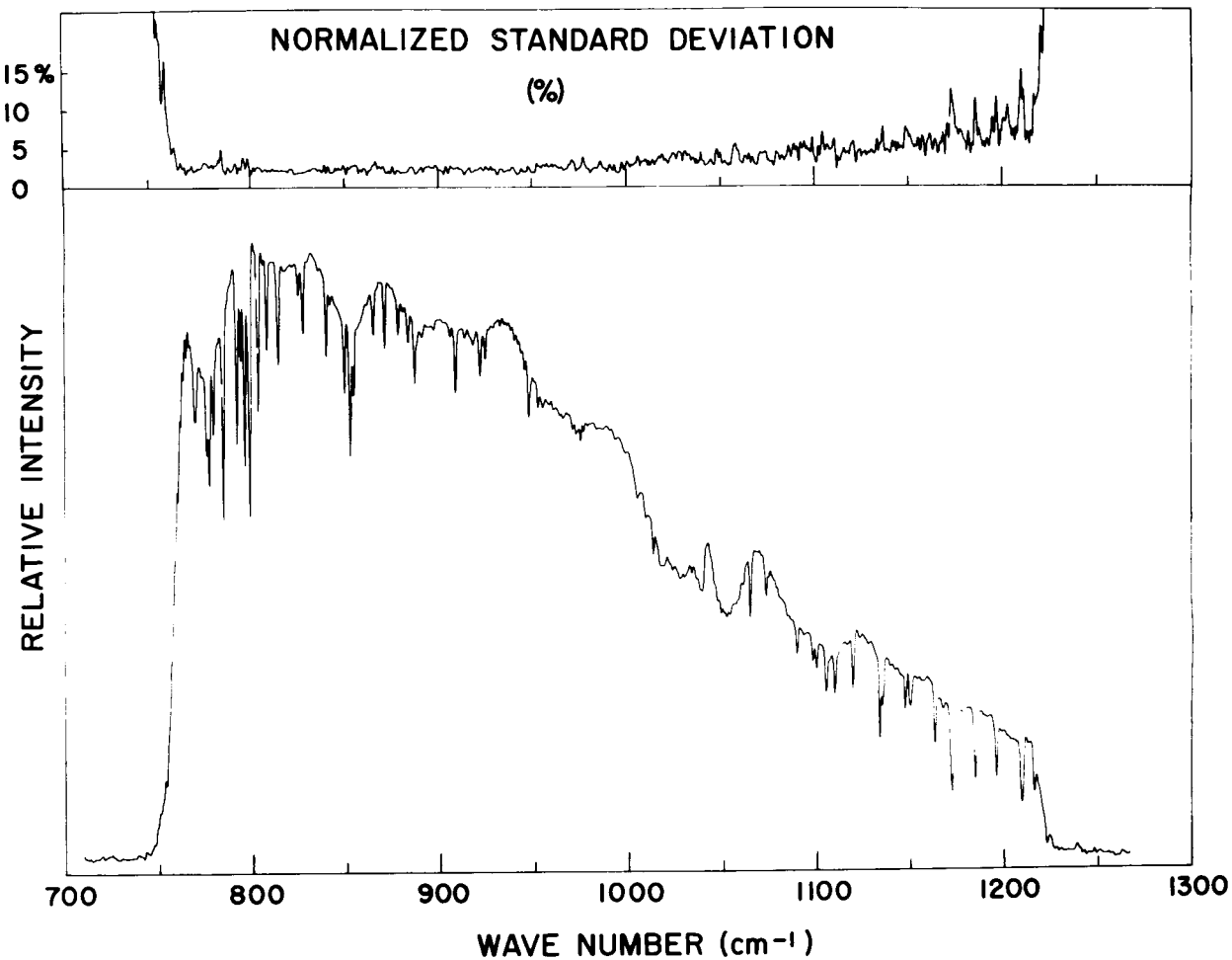

Figure 2. Average spectrum calculated from 16 interferograms and the associated normalized standard deviation;

$$s = \frac{1}{\bar{x}} \sqrt{\frac{\sum_{i=1}^{k} (x_i - \bar{x})^2}{k - 1}}$$

x_i are the individual values of the spectral intensity, $\bar{x}$ the mean value, and $k = 16$ is the number of spectra in the group.

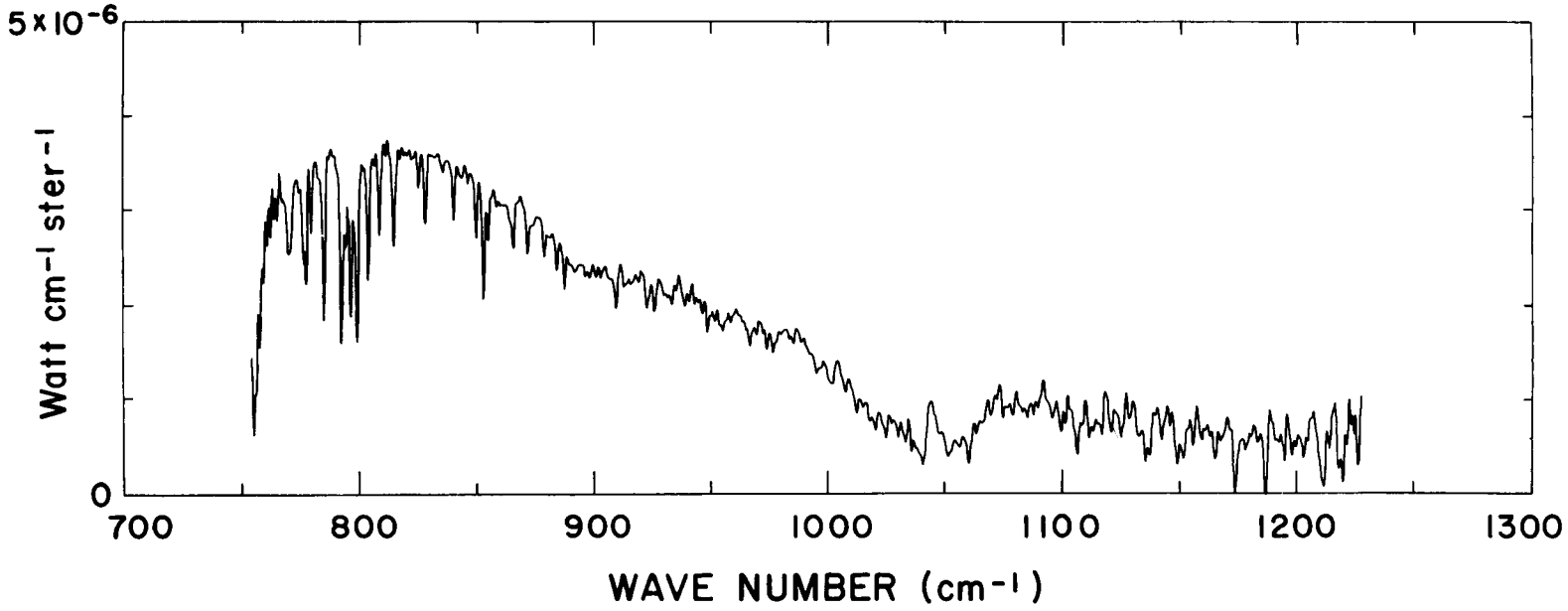

Figure 3. Average difference spectrum calculated from 5 groups of Venus and 5 groups of sky spectra. Normalization to blackbodies provides the absolute calibration. The spectrum has been multiplied by 3.46, the ratio of the field of view to the solid angle of the planet.

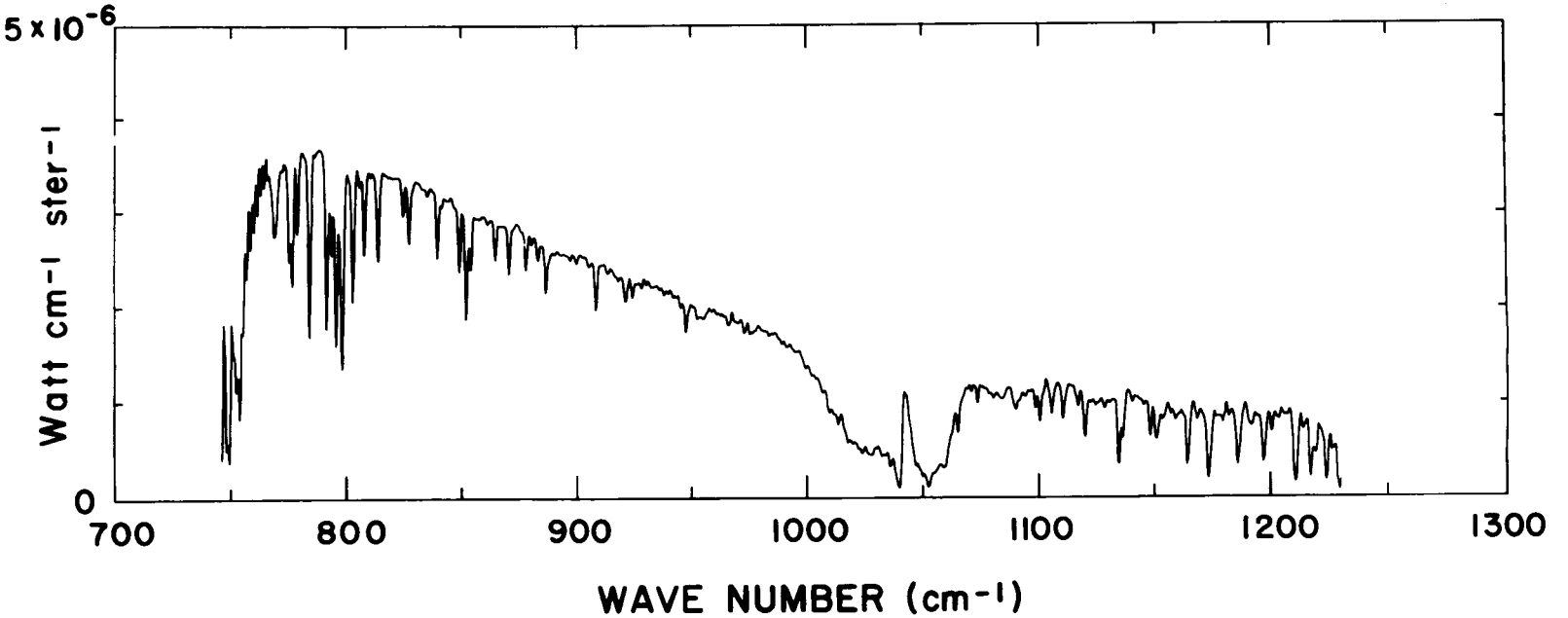

Figure 4. Average difference spectrum of a portion of the moon. Telluric water vapor, carbon dioxide, and ozone lines appear in absorption.

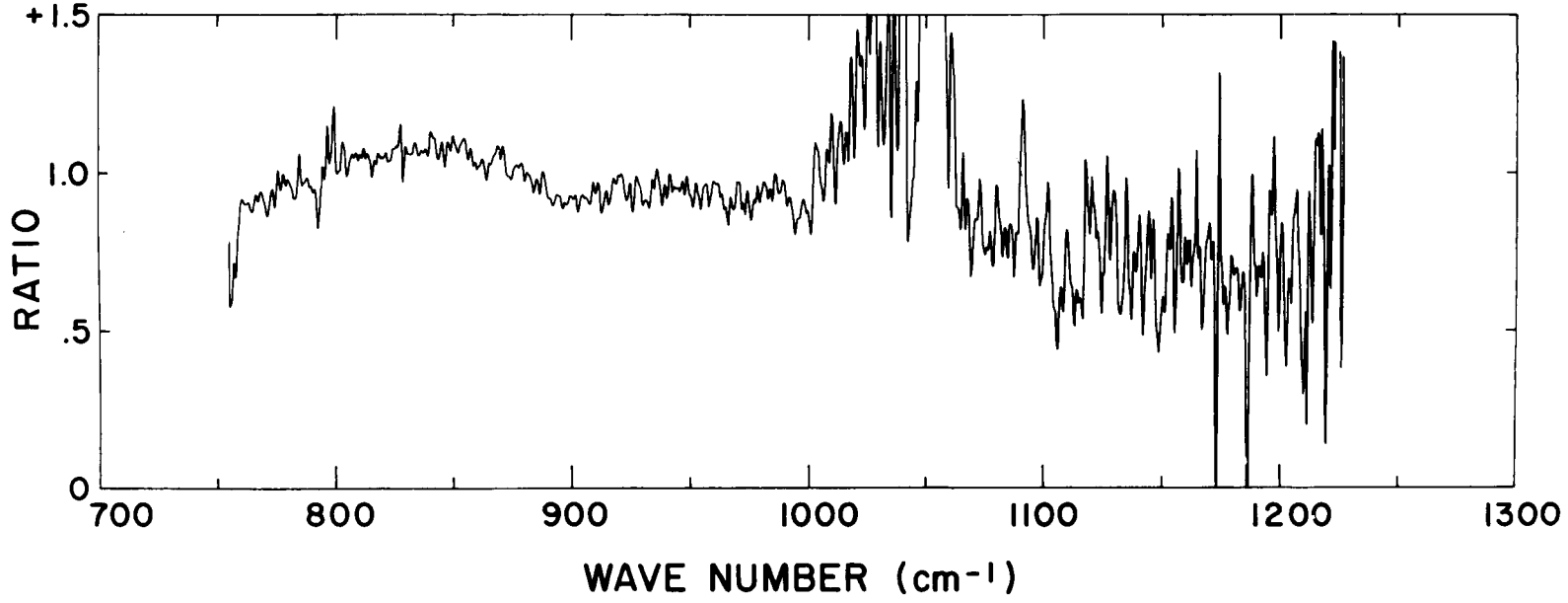

Figure 5. Ratio of the Venus and lunar difference spectra. The region of the strong ozone absorption in the earth's atmosphere (1,000 cm^{-1} to 1,060 cm^{-1}) should be ignored. Noise becomes increasingly stronger towards 1200 cm^{-1}. The broad absorption-like feature near 890 cm^{-1} and the strong 791 cm^{-1} CO_2 absorption may be noticed.

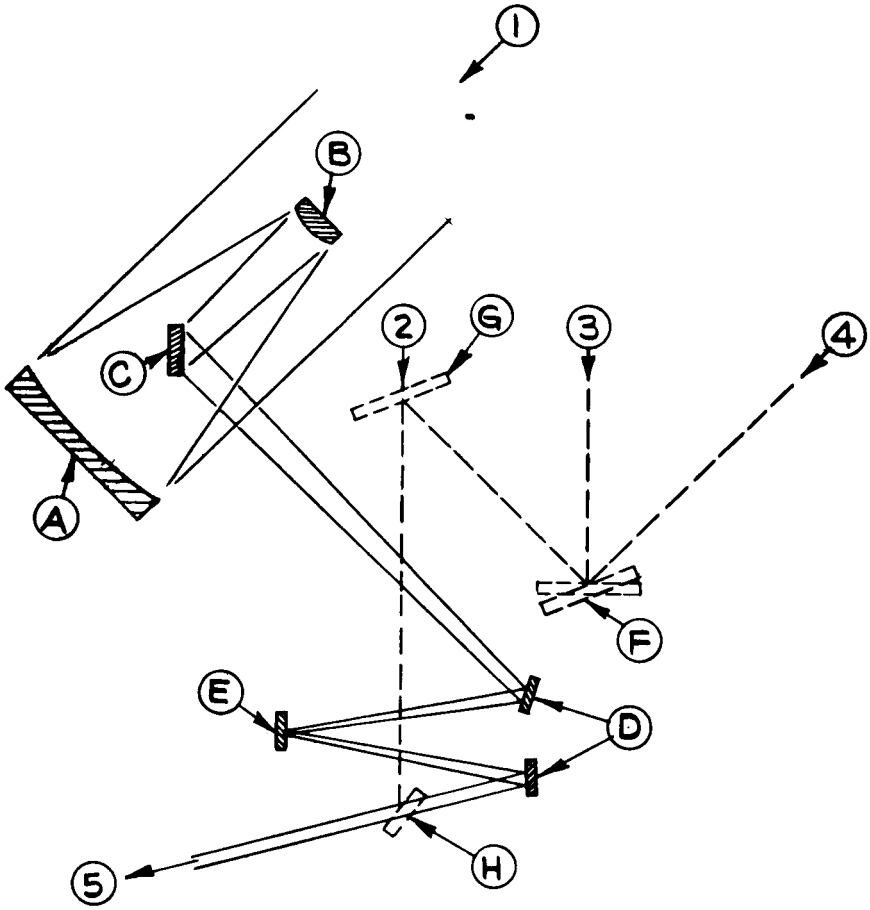

(1) RADIATION FROM SKY (50° ELEVATION)
(2) DIRECT RADIATION FROM SKY (ZENITH)
(3) RADIATION FROM SKY (ZENITH) REFL. BY 2 MIRRORS
(4) RADIATION FROM SKY (50° ELEVATION) REFL. BY 2 MIRRORS
(5) TO INTERFEROMETER
(A) PRIMARY MIRROR
(B) SECONDARY MIRROR
(C) COUDE MIRROR
(D) FLAT MIRRORS, FIXED (GOLD COATED)
(E) FIELD MIRROR AT COUDE FOCUS (GOLD COATED)
(F) FLAT MIRROR, ADJUSTABLE (ALUM. COATED)
(G) FLAT MIRROR, REMOVABLE (ALUM. COATED)
(H) FLAT MIRROR, REMOVABLE (GOLD COATED)

Figure 6. Schematic of the experimental arrangement to determine the telescopic and atmospheric transmission functions. The transmission of the telescope is obtained from a comparison of strong water vapor emission lines in the sky spectra taken with and without the telescope. Atmospheric transmission was calculated from the zenith sky emission and radiosonde data.

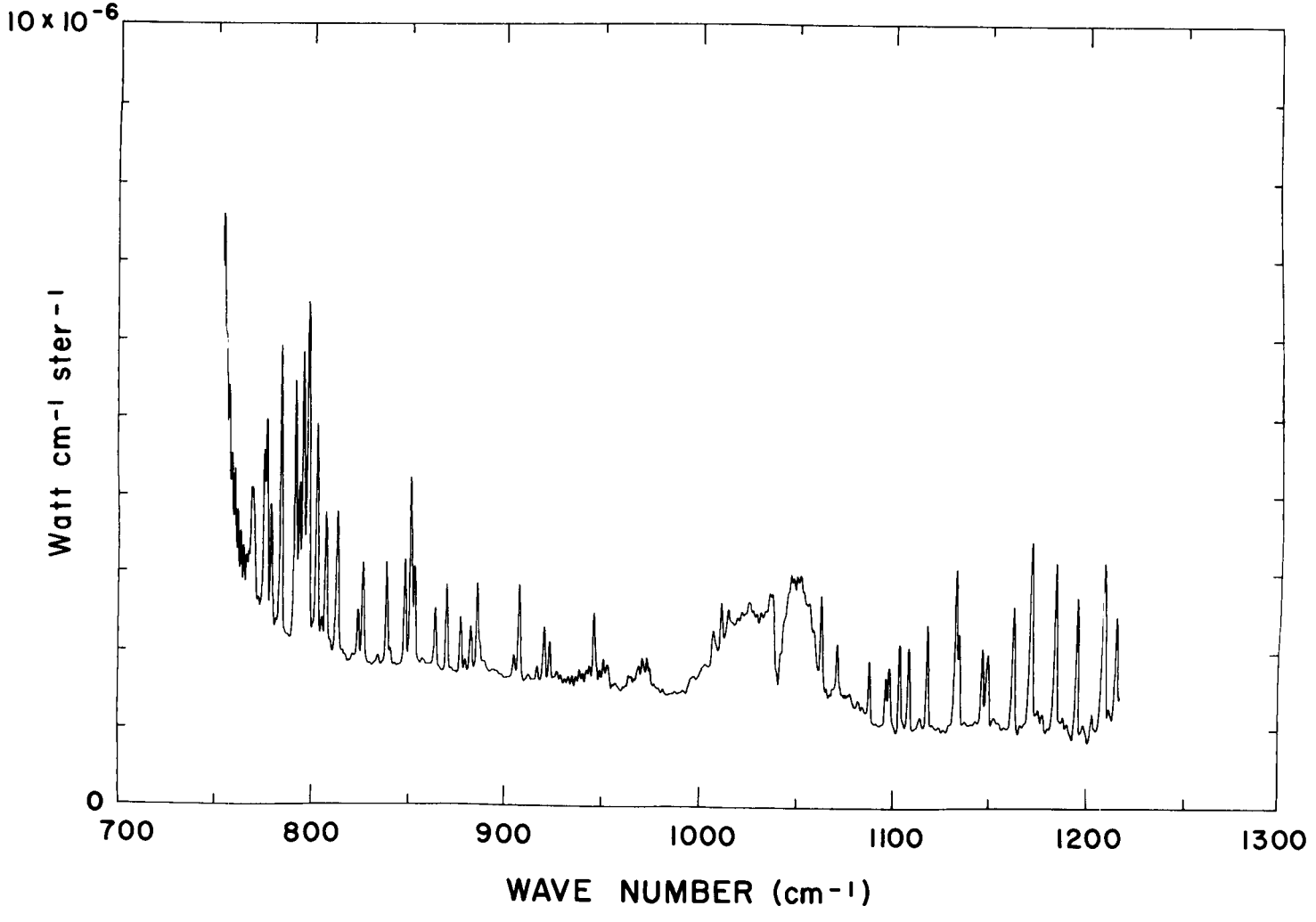

Figure 7. Emission spectrum of the zenith sky. Most lines are due to water vapor except in the region between 1,000 and 1,070 cm^{-1} where ozone bands appear in addition to water vapor emission and in other spectral regions where several bands of CO_2 and N_2O are present. The lines R43 to R61 of the $(\nu_1 - \nu_2)$ CO_2 band and the lines P18 to P36 of the $(\nu_3 - \nu_1)$ CO_2 band are clearly resolved between 754 - 768 cm^{-1} and between 928 - 946 cm^{-1} respectively. The strong CO_2 Q branch near 791 cm^{-1} is also distinct from the adjacent water vapor lines. The $2\nu_2$ N_2O band near 1170 cm^{-1} and the $(\nu_3 - 2\nu_2)$ CO_2 band near 1063 cm^{-1} are less pronounced.

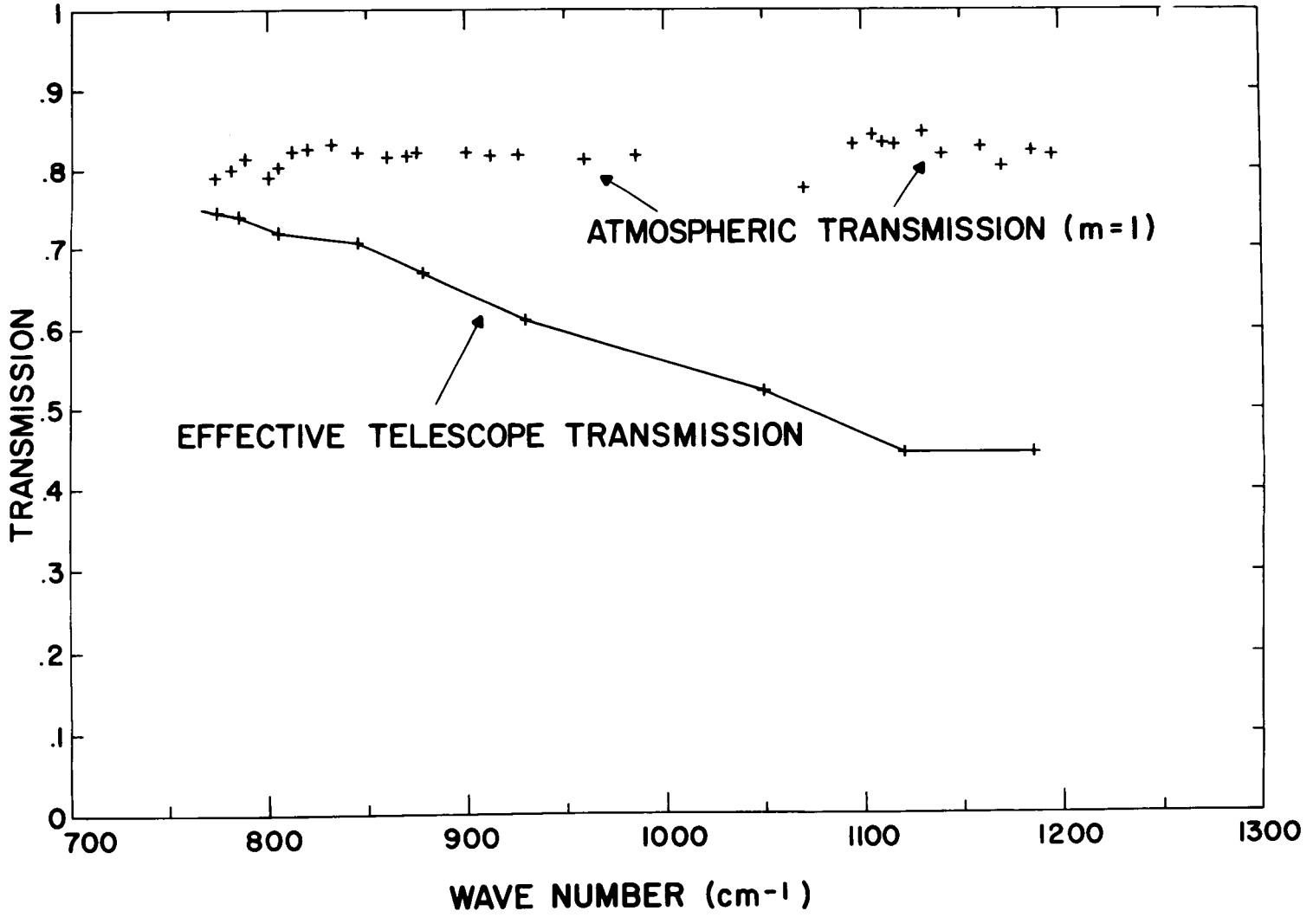

Figure 8. The atmospheric and telescopic transmission functions used. The effects of the water vapor continuum, of weak lines of water vapor and other gases, and of aerosols have been lumped together. The transmission of the telescope was computed from sky spectra. Each point represents the average of 3 to 5 individual measurements of lines near the wave numbers marked.

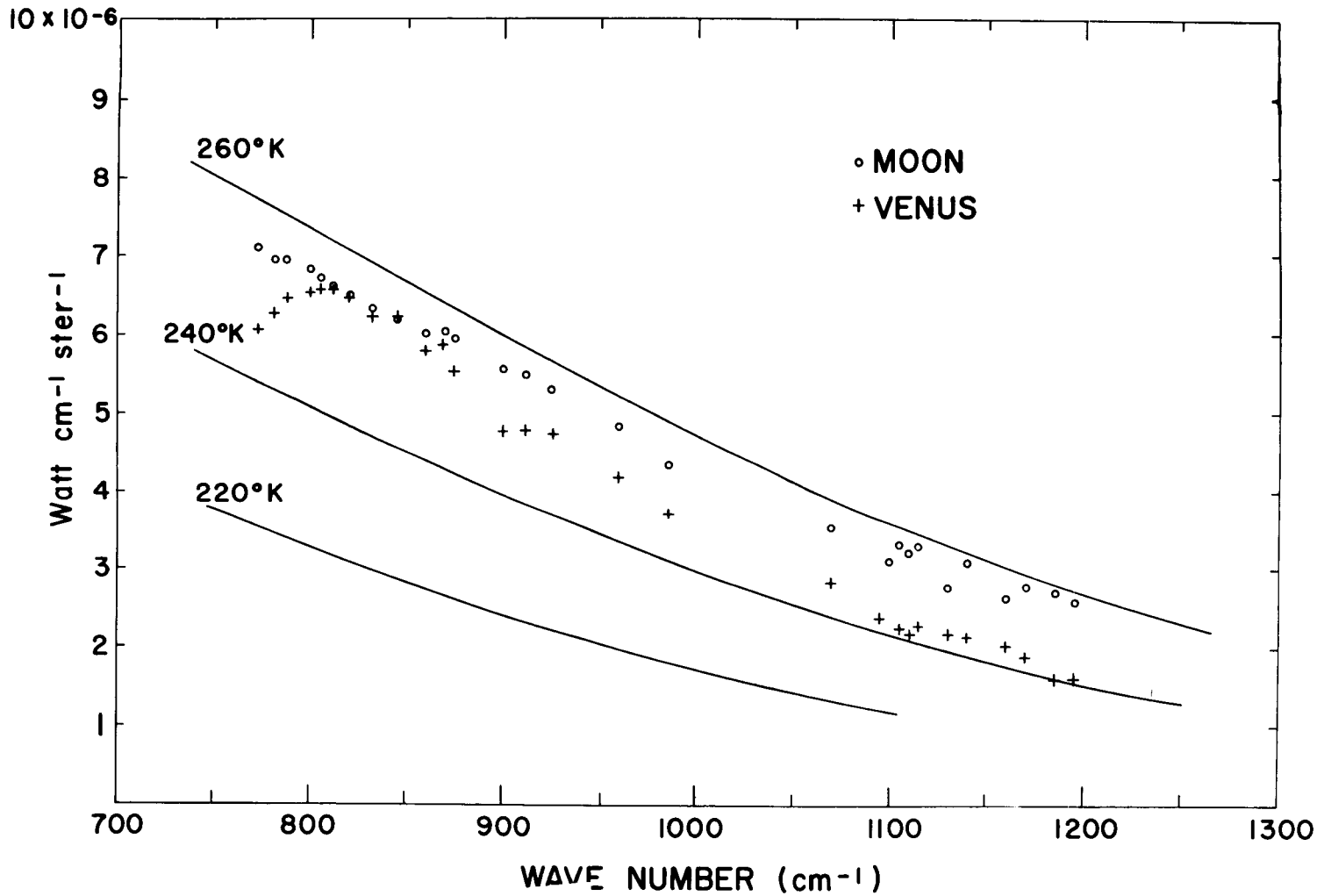

Figure 9. Planetary and lunar intensities. Several curves of constant brightness temperatures are shown for the purpose of comparison. The 890 cm^{-1} absorption-like feature and the general drop in the brightness temperature below 800 cm^{-1} are felt to be significant.